JSE Journal of Systematics and Evolution

doi: 10.1111/jse.12555

Research Article

Genome structure and apomixis in *Phoenicaulis* (Brassicaceae; Boechereae)

Terezie Mandáková[1], Kaylynn Ashby[2], Bo J. Price[2], Michael D. Windham[3], John G. Carman[2], and Martin A. Lysak[1]*

[1]CEITEC, Masaryk University, Brno, CZ-625 00, Czech Republic
[2]Plants, Soils, and Climate Department, Utah State University, Logan, UT 84322-4820, USA
[3]Department of Biology, Duke University, Durham, NC 27708, USA
*Author for correspondence. E-mail: martin.lysak@ceitec.muni.cz. Tel.: 00420 549 494 154.
Received 19 August 2019; Accepted 29 November 2019; Article first published online 10 December 2019

Abstract Apomixis in crucifer (Brassicaceae) species is rare, reported in just four genera (*Boechera*, *Draba*, *Erysimum*, and *Parrya*), and one intergeneric hybrid (*Raphanobrassica*). It is well studied only in *Boechera*, where it is widespread among 100+ recognized species. However, its occurrence in related genera of the tribe Boechereae has not been documented previously. Here we analyzed genome evolution, mode of reproduction, and fertility of the monospecific Boechereae genus *Phoenicaulis* (*P. cheiranthoides*), endemic to the northwestern United States. We discovered that the species encompasses diploid ($2n = 2x = 14$), triploid ($2n = 3x = 21$), and tetraploid ($2n = 4x = 28$) populations. Comparative chromosome painting analyses revealed that the three karyotypes are essentially structurally identical, differing only in the presence of a largely heterochromatic chromosome (*Het*) in the triploid and tetraploid cytotypes. The genome structure of *Phoenicaulis* appeared identical to that of *Boechera* species previously analyzed, suggesting genomic stasis despite the morphological and molecular divergence of the two genera. This genome colinearity extended to the presence and structure of the *Het* chromosomes, which are closely associated with apomictic reproduction in *Boechera*. Interestingly, all three cytotypes of *Phoenicaulis* proved to be apomictic, regardless of the presence or absence of a *Het* chromosome, and sexual populations have yet to be identified.

Key words: apomixis, apospory, autopolyploidy, *Boechera*, Brassicaceae, karyotype evolution.

1 Introduction

Apomixis in seed plants involves asexual seed formation, which can occur either sporophytically or gametophytically. In sporophytic apomixis, embryos form adventitiously in ovules, usually from the nucellar cells of the ovule wall. In most cases, seed development requires the formation of a sexually reduced embryo sac (gametophyte) followed by central cell fertilization, which provides a 3*n* endosperm to nourish the clonal embryo as it develops. The sexual egg or embryo usually aborts (Hand & Koltunow, 2014).

In gametophytic apomixis, a genetically unreduced gametophyte forms as a result of a failed or modified meiosis. Three major types are recognized in eudicots: Antennaria and Taraxacum types of diplospory, which involve gametophyte formation from an ameiotic megaspore mother cell (MMC), and Hieracium type apospory, where the gametophyte forms adventitiously. In Antennaria type diplospory, the MMC produces an unreduced gametophyte directly. In Taraxacum type diplospory, the MMC initiates meiotic prophase, but chromosome synapses and crossing over usually do not occur. A restitution nucleus with condensed univalent chromosomes then forms. Development either proceeds to the second meiotic division, which is mitotic-like (Asker & Jerling, 1992; Crane, 2001), or, as recently suggested by Carman et al. (2019), meiotic abortion during early prophase is complete, and the division reverts at that point to mitosis. In either case, a dyad of unreduced spores is formed, and the gametophyte develops from one of these unreduced spores. In Hieracium type apospory, reversion to asexual development occurs later, generally after meiosis has occurred, whereupon all traces of sexual germline development degenerate. In aposporous plants, support for sexual development fails either during meiosis, shortly after meiosis, or as late as early sexual gametophyte formation (e.g., 1- or 2-nucleate gametophyte stage). One or more unreduced gametophytes then form from nucellar or rarely integument cell(s). In most diplosporous or aposporous eudicot apomicts, the mature gametophyte closely resembles a sexual gametophyte, that is, it forms through three mitotic divisions that produce an 8-nucleate coenocyte. Cellularization then occurs. The two polar nuclei usually fuse to produce the primary endosperm nucleus. The egg in an unreduced apomictic gametophyte develops into an embryo without fertilization (parthenogenetically). In most apomicts, the primary endosperm nucleus must be fertilized for the endosperm to form (pseudogamy). However, in certain species from multiple families, endosperm forms

autonomously, that is, without fertilization (Nogler, 1984; Asker & Jerling, 1992; Hand & Koltunow, 2014).

Apomixis is relatively rare among angiosperms, having been verified in species from only 78 families (19%) and 293 genera (2.2%) (Hojsgaard et al., 2014). However, confirming the presence or absence of apomixis is technically tedious and, without testing for it, there is no way of knowing whether it occurs in untested populations or at untested ploidy levels. In this respect, only a small fraction of the quarter million angiosperm species has been tested, and most of these tests involved limited samplings of species diversity. Accordingly, current numbers of known apomicts may greatly underestimate actual cases, and this is suggested by a 20% increase in numbers of verified apomict-containing genera between 1997 and 2014 (Carman, 1997; Hojsgaard et al., 2014).

Apomixis was first detected in the Brassicaceae in the 1940s when Tyge Böcher noticed that diploid and triploid *Arabis holboellii* (*Boechera holboellii* [Hornem.] Á. Löve & D. Löve, tribe Boechereae) produced unreduced (2*n*) pollen, and the triploids were fully fertile. His subsequent investigations revealed 1*n* pollen and sexual reproduction in diploid *Boechera retrofracta* (Graham) Á. Löve & D. Löve from Alaska and Taraxacum type diplospory in ovules of the 2*n* pollen-forming diploid and triploid *B. holboellii* from Greenland. The mechanism of unreduced spore formation, 1st division restitution, occurred in both ovules and anthers (Bocher, 1951), which is unusual because most apomicts attempt to generate reduced pollen (Asker & Jerling, 1992; Carman, 1997). Subsequent embryological analyses of additional diploid and triploid taxa of *Boechera* Á. Löve & D. Löve from the western United States, mostly 2*n* pollen-forming plants, also revealed reproduction by Taraxacum type diplospory (Naumova et al., 2001; Taskin et al., 2004; Carman, 2007; Sharbel et al., 2010; Rojek et al., 2018). However, *B. microphylla* (Nuttall) Dorn, which was previously considered sexual because it often produces predominantly 1*n* pollen, was found to be highly aposporous (Carman, 2007). Recently, 44 *Boechera* species and hybrids were studied embryologically, of which 18 were sexual, 16 were diplosporous, 19 were aposporous, and seven were aposporous and diplosporous. In general, the diplosporous apomicts produced 2*n* pollen, and the aposporous apomicts produced 1*n* pollen (Carman et al., 2019).

In addition to *Boechera*, Mulligan (1966) reported apomixis in *Erysimum* L. (tribe Erysimeae) and Mosquin & Hayley (1966) noted its occurrence in *Parrya* R. Brown (tribe Chorisporeae). Hybridization studies (Mulligan & Findlay, 1970) and embryological and single seed flow cytometry analyses (Jordon-Thaden & Koch, 2012) suggest that *Draba oligosperma* Hooker (tribe Arabideae) is also apomictic and possibly aposporous. And finally, high-frequency apospory (36–70% of ovules) was observed in synthetic *Raphanus* × *Brassica* hybrids (tribe Brassiceae) (Ellerstrom & Zagorcheva, 1977; Ellerstrom, 1983). Collectively, these studies involving five different tribes of Brassicaceae suggest that apomixis has evolved independently multiple times within the family.

Though apomixis in *Boechera* has been researched for decades, surprisingly little is known about the reproductive modes of its closest relatives. The monophyletic tribe Boechereae harbors eight genera and ca. 130 species endemic to North America and the Russian Far East (Al-Shehbaz, 2012; Alexander et al., 2013). Herein, we report analyses of genome evolution and mode of reproduction in the genus *Phoenicaulis* Nutt., currently treated as a single species (*P. cheiranthoides* Nutt.) though several other species have been recognized in the past. The genus is widely distributed in the northwestern United States, occurring in rocky montane habitats at elevations ranging from 700 to 2800 m. Previously, the species was known to be tetraploid ($2n = 4x = 28$) based on a single count published in the *Flora of North America* (Al-Shehbaz, 2010). Recently, however, we identified diploid ($2n = 2x = 14$) and triploid ($2n = 3x = 21$) populations of *P. cheiranthoides*. Here, we report results of chromosome painting analyses, designed to elucidate the origins and genome evolution of *Phoenicaulis*, and cytoembryological analyses, which were used to characterize modes of reproduction.

2 Material and Methods

2.1 Plant material

Five populations of *Phoenicaulis cheiranthoides* were fully analyzed: Lobdell Lake (38.4446°N, 119.3492°W; *Windham et al. 4526*, June 8, 2018; Fig. 1), Masonic Mt. (38.3476°N, 119.1287°W; *Windham et al. 4522*, June 7, 2018), Aurora Canyon (38.2759°N, 119.148°W; seeds obtained from Millennium Seed Bank, MSB 0196750); Bishop Creek (37.2329°N, 118.5963°W; *Windham et al. 4510*, June 6, 2018), and Angel Lake (41.0249°N, 115.0885°W; *Windham 3097*, May 27, 2004). An additional population was included in the embryological studies but not karyotyped: Big Indian (42.6722°N, 118.6904°W; *Windham 3129*, June 1, 2004). Plants of the Aurora Canyon population were grown from seed. Specimens of the remaining populations were collected in the field. Herbarium vouchers for all field collections are deposited in the Duke University Herbarium (DUKE). Whole young inflorescences from different individuals were fixed in freshly prepared ethanol: acetic acid (3: 1) overnight, transferred into 70% ethanol and later stored at −20 °C until use.

2.2 Chromosome spreads

Mitotic and meiotic chromosome spreads were prepared from anthers of young flower buds (Mandáková & Lysak, 2016a). On average, ten different inflorescences originating from several plants were used for chromosome spreads. Briefly, after washing in citrate buffer (10 mM sodium citrate, pH 4.8), selected flower buds were digested using a 0.3% mix of pectolytic enzymes (cellulase, cytohelisase, pectolyase) (Sigma-Aldrich Corp., St. Louis, MO, USA) in citrate buffer for ca. 3 h. Individual anthers were dissected and spread in 20 µL of 60% acetic acid on a microscope slide placed on a metal hot plate (50 °C), fixed by ethanol: acetic acid (3:1) and the slide was dried using a hairdryer. Suitable slides were postfixed in freshly prepared 4% formaldehyde in distilled water for 10 min and air-dried.

2.3 rDNA and telomeric probes

The *Arabisopsis thaliana* (L.) Heynh. bacterial artificial chromosome (BAC) clone T15P10 (AF167571) containing 35S rRNA genes was used for *in situ* localization of nucleolar

Fig. 1. Diploid plants of *Phoenicaulis cheiranthoides* (Lobdell Lake). Photographs by T. Mandáková (June 8, 2018).

organizer regions (NORs), and the *A. thaliana* clone pCT4.2 (M65137), corresponding to a 500 bp 5S rDNA repeat, was used for localization of 5S rDNA loci. The *Arabidopsis*-type telomere repeat (TTTAGGG)*n* was prepared according to Ijdo et al. (1991).

2.4 Comparative chromosome painting and chromosomal localization of repeat probes

Arabidopsis BAC contigs, corresponding to 22 genomic blocks (Lysak et al., 2016), were used as chromosome-specific painting probes following the chromosome structure of *Boechera* species (Mandáková et al., 2015). The first and last BAC clones of each contig are listed in Fig. 2A. Isolated BAC DNAs and/or repeat probes were labeled with Cy3-, biotin-, or digoxigenin-dUTP by nick translation, as described by Mandáková & Lysak (2016b). The labeled probes were then pooled, ethanol-precipitated, desiccated, and dissolved in 20 µL of 50% (v/v) formamide and 10% (v/v) dextran sulfate in 2 × SSC per slide overnight. The probes were denatured together with chromosome-containing slides on a hot plate at 80 °C for 2 min, hybridized overnight at 37 °C, and washed in 20% formamide in 2 × SSC at 42 °C. The immunodetection of hapten-labeled probes was performed as described by Mandáková & Lysak (2016b).

After immunodetection, the preparations were stained with 4′,6-diamidino-2-phenylindole (DAPI; 2 µg/mL) in Vectashield (Vector Laboratories, Peterborough, UK). Fluorescence signals were analyzed using an Axioimager Z2 epifluorescence microscope (Zeiss, Oberkochen, Germany) and CoolCube CCD camera (MetaSystems, Newton, MA, USA). Images were acquired separately for the four fluorochromes using appropriate excitation and emission filters (AHF Analysentechnik, Tübingen, Germany). The three monochromatic images were pseudocolored and merged using Adobe Photoshop CS6 software (Adobe Systems, San Jose, CA, USA).

2.5 Embryology

Clusters of floral buds at pre-anthesis stages were fixed in 3:1 fixative for 48 h. The buds were then cleared in 2:1 benzyl benzoate dibutyl phthalate (BBDP) (Crane & Carman, 1987) as follows: 70% EtOH, 30 min; 95% EtOH, 4 h (2x); 2:1 95% EtOH BBDP, 2 h; 1:2 95% EtOH BBDP, 4 h; 100% BBDP, 4 h; and 100% BBDP overnight (kept until analyzed). Pistils were then dissected from the floral buds, measured from the base of the pedicel to the top of the stigma (±0.05 mm), and mounted on slides with a minimal amount of 2:1 BBDP clearing solution. An Olympus (Center Valley, PA, USA) BX53 microscope equipped with differential interference contrast (DIC) optics, an Olympus DP74 digital camera, and Olympus cellSens Dimension Version 1 software was used to investigate parietal cell formation, MMC formation, megasporogenesis, fate of meiotic spores, and the cellular origins of female gametophytes. Enlarged 1- or 2-nucleate functional megaspores that possessed one or more large vacuoles were scored as coenocytic (immature) sexual gametophytes. Likewise, enlarged 1- or 2-nucleate nucellar cells that possessed one or more large vacuoles were scored as immature aposporous gametophytes. Because of uncertainties in origin, gametophytes were not scored as sexual or apomictic if they had developed beyond the 2-nucleate stage. Pistil length and the developmental stage of the majority of scorable ovules in each pistil were recorded.

2.6 Pollen fertility

Selected flower buds containing yellow anthers, fixed in 3:1 fixative and stored in 70% ethanol, were thoroughly washed in distilled water and stained using the Alexander stain solution (Alexander, 1969) for 10 to 15 min. The buds were dissected to release the anthers and pollen, and stained pollen grains were observed and photographed using an AxioLab A1 light microscope equipped by an AxioCam 105 camera (Zeiss). Pollen grains were measured using the ImageJ program (National Institutes of Health).

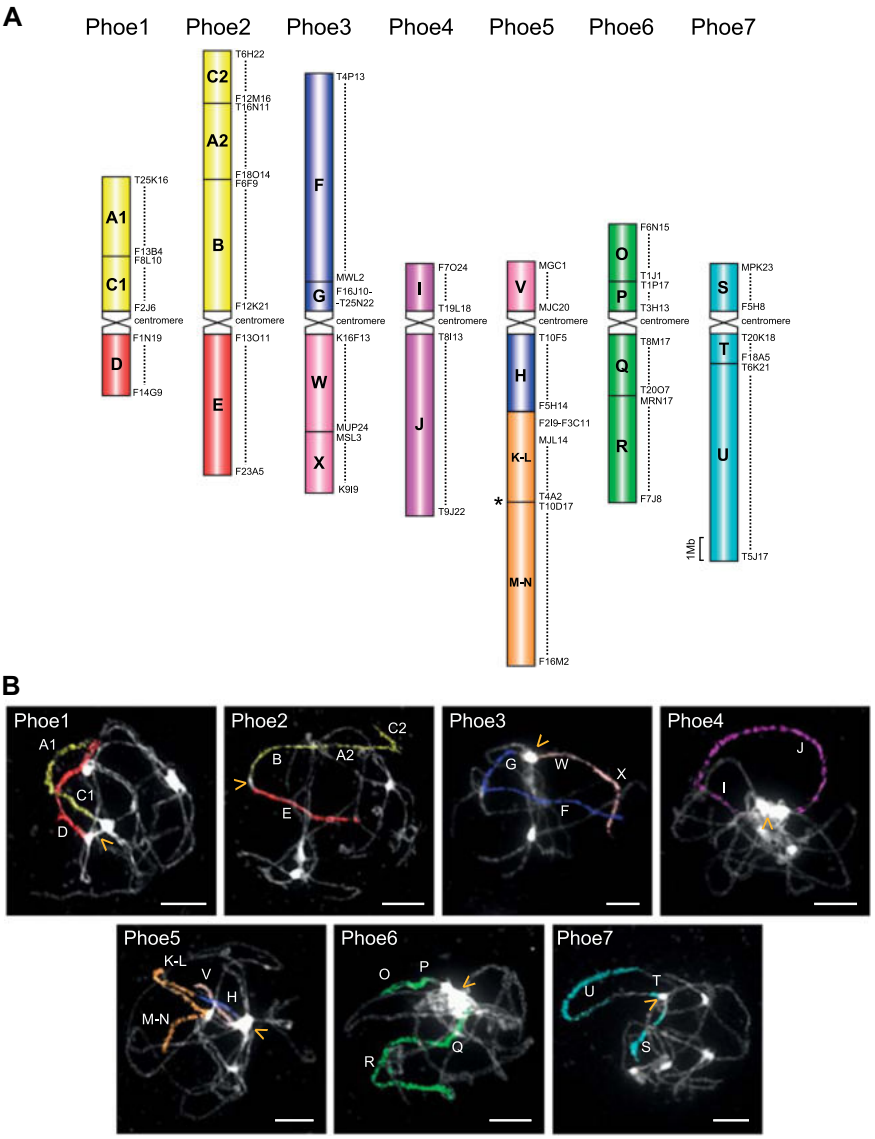

Fig. 2. Genome structure of diploid *Phoenicaulis cheiranthoides* ($n = 7$) based on comparative chromosome painting (CCP) analysis. **A,** The purported origin of the *P. cheiranthoides* genome from Ancestral Crucifer Karyotype ($n = 8$) and comparative cytogenomic map of *P. cheiranthoides* based on CCP data (see **B**). The different colors correspond to the eight ancestral chromosomes of Ancestral Crucifer Karyotype (ACK), whereas capital letters refer to 22 genomic blocks (A–X). *Arabidopsis* bacterial artificial chromosome (BAC) clones defining each genomic block/painting probe are listed along the chromosomes. The star symbol indicates a putatively inactive paleocentromere on chromosome Phoe5. **B,** Painting of the seven *Phoenicaulis* chromosomes using *Arabidopsis* BAC contigs (as defined in [**A**]) on pachytene chromosome spreads. Chromosomes were counterstained with DAPI. The fluorescence of painting probes was captured as black and white photographs and signals were pseudocolored to match the eight chromosomes of ACK. Centromeres are labeled by arrowheads. Scale bars, 10 μm.

3 Results

3.1 Chromosome counts and ploidy levels

Five populations of *Phoenicaulis cheiranthoides* were analyzed karyologically. The Lobdell Lake population (Fig. 1) was diploid ($2n = 2x = 14$), two populations (Masonic Mt. and Aurora Canyon) were triploid ($2n = 3x = 21$) and two (Bishop Creek and Angel Lake) were tetraploid ($2n = 4x = 28$). The Big Indian population (included in the embryological studies but not karyotyped) was tetraploid as well. After DAPI staining of mitotic chromosome spreads, a single chromosome with brightly fluorescing DAPI signal was observed among chromosomes of the triploid and tetraploid, but not among chromosomes of the diploid.

3.2 Karyotype structure

Bacterial artificial chromosome-based comparative chromosome painting was used to reveal the genome structure among the three cytotypes. Probes were arranged according

to the genome structure of *Boechera* (Mandáková et al., 2015), and all of the 22 crucifer genomic blocks (Lysak et al., 2016) were mapped to *Phoenicaulis* chromosomes (Phoe1–Phoe7) (Fig. 2). Interestingly, the seven chromosomes of diploid *Phoenicaulis* show perfect collinearity with the seven chromosomes of diploid *Boechera* (Mandáková et al., 2015). This inter-generic collinearity corroborates the origin of the most recent common ancestor of both genera from Ancestral Crucifer Karyotype (ACK, $n = 8$; Fig. 2A), as inferred for the ancestral *Boechera* genome earlier (Mandáková et al., 2015). Three and four copies of the seven *Phoenicaulis* chromosomes were observed in the triploid and tetraploid cytotypes, respectively (Figs. 3A–3C). Chromosome rearrangements that might differentiate *Phoenicaulis* cytotypes or *Phoenicaulis* from *Boechera* were not detected.

Ribosomal RNA genes were localized to three chromosomes (Figs. 3A–3C). Nucleolar organizer regions (NORs, 35S rDNA loci) were localized to two, three, and four Phoe6 homologs among the diploid, triploid, and tetraploid cytotypes, respectively. Two 5S rDNA loci were localized to Phoe5 and Phoe7 homologs. Comparative painting with probes specific to Phoe1 revealed differences among the three ploidies (Figs. 3D–3F). In the diploids, both homologs are of comparable size and morphology (Fig. 3D). However, in the triploid and tetraploid cytotypes, one of the three or four homologs is larger with a considerably expanded pericentromeric region (Figs. 3E, 3F). This single chromosome is referred to herein as a *Het* (heterochromatic) chromosome.

3.3 The Het chromosome during microsporogenesis

We were unsuccessful in analyzing chromosome pairing behavior of the *Het* chromosome in the tetraploid. Hence, our observations are limited to pollen mother cells of triploid plants. At pachytene, the three Phoe1 homologs usually formed an apparent trivalent, with two homologous bottom arms (block D, red) synapsed as a bivalent and the third homolog presumably intimately aligned with them. The upper arms often continued this two-by-one pairing proximally (proximal regions of block C1, yellow) but with one homologous arm failing to pair and the other two arms pairing distally (distal region of block C1 and entire block A1, green) (Fig. 3G). Trivalents dissociated in later phases of prophase I, and a bivalent and one univalent were regularly observed during diakinesis (Fig. 3H) and anaphase I (Fig. 3I). During the first meiotic division, the two Phoe1 homologues and the *Het* chromosome could not be distinguished based on pericentric heterochromatin. Hence, we were unable to determine if the *Het* chromosome forms the univalent or participates in forming a bivalent (Figs. 3G–3I).

3.4 Embryology

Megasporogenesis and the definitive stages for determining the cellular origin of gametophytes (1–2 nucleate gametophyte stage) occurred in pistils that measured 1.0–2.4 mm in length. Numbers of available pistils in this range were 16, 43, 74, and 83 for the Lobdell Lake, Masonic Mt., Angel Lake and Big Indian collections, respectively, and these were analyzed. Two ovule development criteria were used to confirm gametophytic apomixis: (i) absence of sexual gametophyte formation (from a megaspore of a meiotic tetrad) and (ii) onset of gametophyte formation either directly from the MMC (Antennaria type diplospory), a spore of an apomeiotic dyad of megaspores (Taraxacum type diplospory), or a cell of the nucellus or integument (apospory). Diplospory was not observed in any of the taxa. In contrast, all 25 of the 1–2 nucleate gametophytes observed in ovules of the diploid cytotype were of aposporous origin, and 26 of 27 1–2 nucleate gametophytes in the tetraploids were of aposporous origin. Further studies are necessary to document the latter stages of aposporous gametophyte maturation in *Phoenicaulis*. In contrast, only 40% of ovules of the triploid were producing aposporous gametophytes (Fig. 4). The remaining 60% initiated gametophyte formation, without apospory, from the surviving megaspores of meiotically derived tetrads. Presumably, these gametophytes were genetically imbalanced due to the random segregation of univalents during megasporogenesis.

The nucellus in the ovules of angiosperms forms by periclinal divisions of subepidermal cells (L2 layer) in the chalazal region of the young funiculus (Johri et al., 1992; Dwivedi et al., 2014). These divisions produce stacks (columns) of cells that extend from the chalaza to the distal micropylar end of the nucellus (Fig. 5A). Hence, the nucellus, excluding its epidermis, is of L2 origin. Anticlinal cell divisions of the prenucellar chalazal epidermis (L1 layer) produce the nucellar epidermis, which is thus of L1 origin. Cell expansion in the nucellar epidermis pulls adjoining subepidermal nucellar cells distally, which causes their periclinal division planes to appear tilted (Fig. 5A). A unique feature of ovule development in *P. cheiranthoides*, at all three ploidy levels, was the prevalence of parietal cells, which occurred in 80–90% of the ovules. Parietal cells belong to the central most column of nucellar cells and form between the nucellar epidermis and the MMC.

The archesporial cell differentiates from the distal-most cell of the central column of nucellar cells. Hence, it is, at least initially, located against the nucellar epidermis at the micropylar end of the nucellus. A parietal cell, the presence of which is of taxonomic significance (Johri et al., 1992), forms when the archesporial cell undergoes a periclinal mitotic division rather than developing directly into the MMC. The distal and proximal cells of this division become the parietal cell and the MMC, respectively. Parietal cells in some angiosperms undergo additional mitotic divisions to produce a parietal tissue of two or more cells, which further positions the MMC deeper within the ovule. A single division of the parietal cell occurred frequently in *P. cheiranthoides* ovules, the division plane being either periclinal (Figs. 5A, 5B, 5E) or anticlinal (Figs. 5C, 5D). Most of these parietal cells expanded in size and some of them produced aposporous gametophytes (Figs. 5B, 5E, 5F, S1, S2).

3.5 Pollen fertility

We analyzed pollen fertility in all three cytotypes (Table S1; Fig. S3). In the diploids, pollen fertility was almost 98%, whereas in the triploids only 50% of pollen were scored as being fertile. The tetraploid cytotype showed intermediate pollen fertility (71%). Based on the observed formation of bivalents and univalents during meiosis I (Figs. 3H, 3I), the reduced pollen fertility in the triploid can be linked to the random segregation of univalents during microsporogenesis.

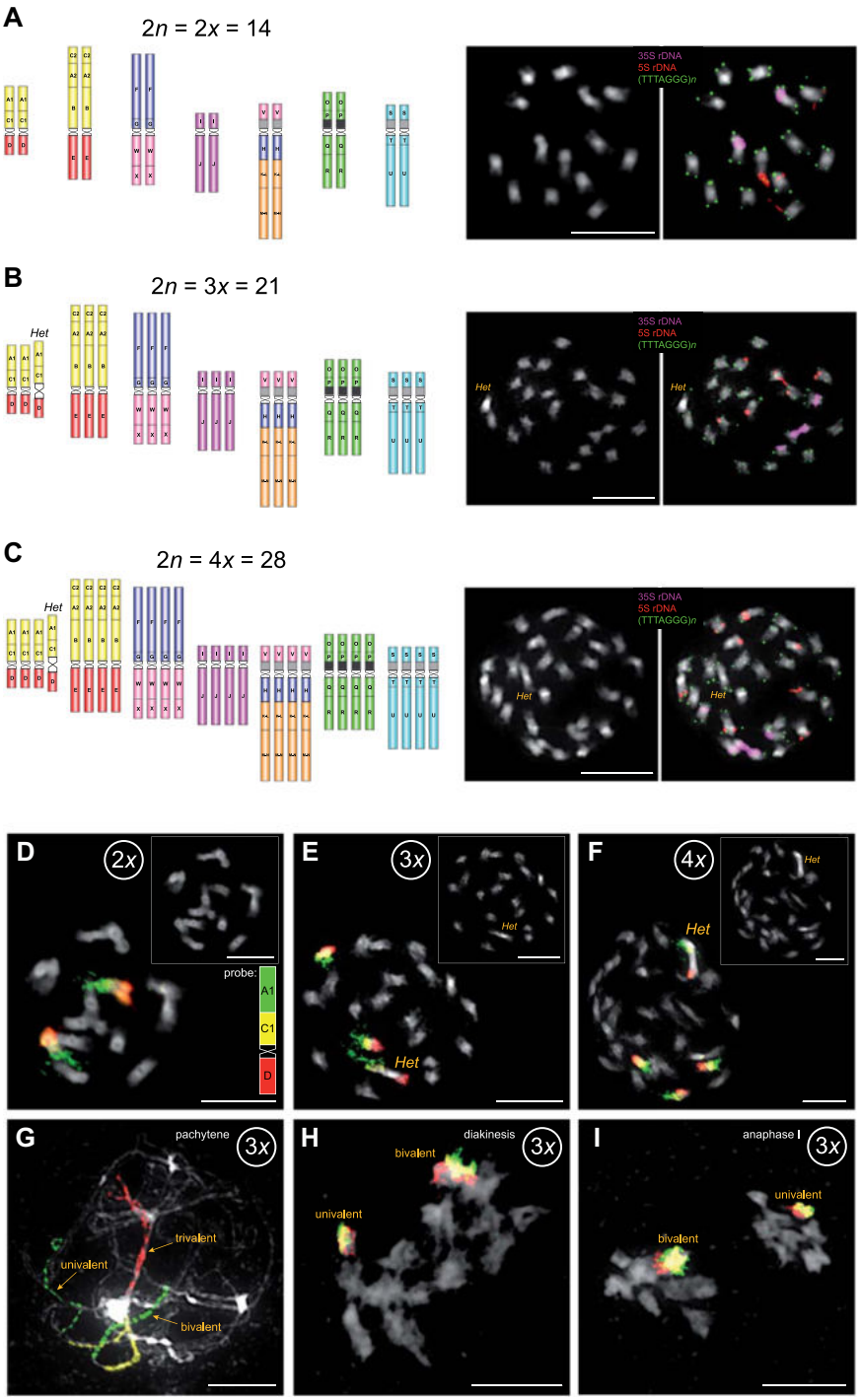

Fig. 3. Comparative genome structure and chromosomal features of the three cytotypes of *P. cheiranthoides*. **A–C,** Comparative genome structure of the three cytotypes and *in situ* localization of rDNA loci and telomeric repeats on mitotic chromosomes. **D–F,** Comparative chromosome painting with three probes specific for chromosome Phoe1 (see Fig. 2A) on mitotic chromosome spreads in the diploid **(D)**, triploid **(E)** and tetraploid **(F)** cytotypes, respectively. In the triploid cytotype **(E)**, painting probes identified two Phoe1 homologues and the heterochromatic *Het* chromosome. In the tetraploid cytotype **(F)**, the same probe labeled three Phoe1 homologues and the *Het* chromosome. **G–I,** Pairing of Phoe1 homologues and *Het* during the first meiotic division in pollen mother cells of the triploid cytotype. The Phoe1-specific painting probes revealed the predominant formation of a bivalent and one univalent (*Het*) at pachytene **(G)**, diakinesis **(H)** and anaphase I **(I)**. Scale bars, 10 μm.

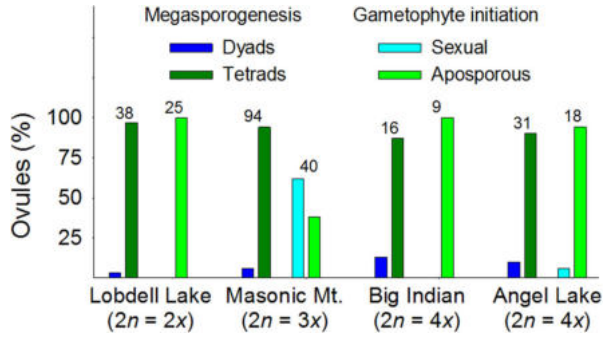

Fig. 4. Sexual dyad and tetrad frequencies and sexual and aposporous gametophyte frequencies observed among appropriately-staged ovules of diploid, triploid and tetraploid cytotypes of *Phoenicaulis cheiranthoides*. Numbers of informative ovules analyzed appear above each set of bars.

4 Discussion

4.1 *Phoenicaulis* and *Boechera* genomes are structurally identical and originated from a common *n* = 7 ancestor

The identical structure of seven chromosomes in *Boechera* and *Phoenicaulis* corroborates the hypothesis that the base number reduction (from $x = 8$ to $x = 7$, Fig. 2A) in an ancestral Boechereae genome occurred very early in the evolution of the tribe (Mandáková et al., 2015) as well as the strongly supported monophyly of the Boechereae (Alexander et al., 2013). As *Boechera* and *Phoenicaulis* genomes share three chromosomes with Ancestral Crucifer Karyotype (ACK, $n = 8$) and the origin of the remaining four chromosomes can be easily reconstructed from five chromosomes of ACK (Mandáková et al., 2015), an ACK-like genome with eight chromosomes was most likely an immediate ancestor of the ancestral $n = 7$ genome of the Boechereae. This is further supported by identifying an ACK-like genome as the most probable ancestral genome of the tribe Halimolobeae (Mandáková et al., 2017), repeatedly retrieved as a sister clade to the Boechereae (Alexander et al., 2013; Mandáková et al., 2017; Nikolov et al., 2019).

4.2 Three cytotypes of *Phoenicaulis*

Our analysis revealed that the currently monospecific genus *Phoenicaulis*, endemic to the northwestern United States, is not uniform karyologically. Instead, three ploidy levels were identified within the species range. The conserved structure of all seven chromosomes across the three ploidies suggests an autopolyploid relationship among all three cytotypes. This is further supported by rDNA loci localized on the same homologous chromosome sets, with their numbers corresponding to the respective ploidy levels. Due to limited population sampling, the geographic pattern of the three cytotypes and their single vs. recurrent origin(s) remain to be established, but our preliminary data suggest that the tetraploid is more broadly distributed than the other two cytotypes.

4.3 Implications of a *Het* chromosome in *Phoenicaulis*

A single *Het* chromosome, with a significantly larger pericentromeric heterochromatin region, was observed in the triploid and tetraploid cytotypes of *Phoenicaulis*. A similar chromosome is strongly associated with the occurrence of diplosporous apomixis in *Boechera* (Sharbel et al., 2004; Kantama et al., 2007; Mandáková et al., 2015). Interestingly, the *Het* chromosomes in *Boechera* (Mandáková et al., 2015) and *Phoenicaulis* belong to the same homologous set. Contrary to diplosporously apomictic diploid *Boechera* ($2n = 14$), with one homolog of chromosome 1 being *Het*, both homologues of chromosome 1 show a comparable size and morphology in diploid *Phoenicaulis*. A *Het* chromosome homologous to chromosome 1 found in triploid and tetraploid cytotypes but allegedly absent in diploid plants has multiple implications.

Based on the presence of only one *Het* chromosome in triploids and tetraploids, the origin of the triploid cytotype ($2n + 1n$) can be inferred as a merger of an unreduced $2n$ gamete with a reduced one ($1n$) gamete, whereas the tetraploid cytotype ($4x$) may have originated from a triploid plant after fertilization of an unreduced triploid egg ($2n = 3x$) by a haploid sperm ($1n = 1x$). As in *Boechera*, the *Het* chromosome in *Phoenicaulis* might be linked to diplospory-related genes on this chromosome (triploids and tetraploids), but not to apospory (diploids). Then, the origin (heterochromatinization) of *Het* in the triploid and tetraploid cytotypes might have been triggered by intraspecific hybridization, that is, by a merger of unreduced ($2n = 2x$ or $3x$) and reduced ($1n = 1x$) gametes. However, the absence of a *Het* chromosome in the diploids and the presence of only a single *Het* chromosome in the triploids and tetraploids suggests another possible origin for *Phoenicaulis*. Here, the *Het* chromosome may have originated from an unreduced gamete of a diploid apomict (presumably a common progenitor of *Boechera* and *Phoenicaulis*) that contained a single *Het* chromosome. This *Het* containing gamete may have then fused with an unreduced gamete of a genomically similar diploid that lacked the *Het* chromosome. Accordingly, *Phoenicaulis* would have originated as a tetraploid. Diploid *Phoenicaulis* may have then formed by parthenogenesis of a reduced egg that lacked a *Het* chromosome. Such haploid parthenogenesis occurs at low frequencies among many apomicts (Asker & Jerling, 1992; Carman et al., 2019). Triploid cytotypes would have then formed as suggested above. For the diploids, a tetraploid origin for *Phoenicaulis* explains the absence of a *Het* chromosome, the absence of sexual reproduction, and the presence of apomixis. Furthermore, it suggests that the *Het* chromosome may be an artifact of apomixis rather than a cause. This possibility requires further investigation involving diplosporous and aposporous *Boechera*.

4.4 Ovule development in *Phoenicaulis*

In tenuinucellate development, the archesporial cell differentiates directly into an MMC against the nucellar epidermis at the micropylar end. However, in our samples of *P. cheiranthoides*, the archesporial cell usually divided mitotically to produce a parietal cell distally and the MMC proximally. This is more typical of crassinucellate development (Johri et al., 1992). Additionally, the parietal cell often divided periclinally or anticlinally to produce a parietal tissue consisting of two cells (Fig. 5). While single parietal cells are somewhat common in *Boechera*, occurring in 30–50% of

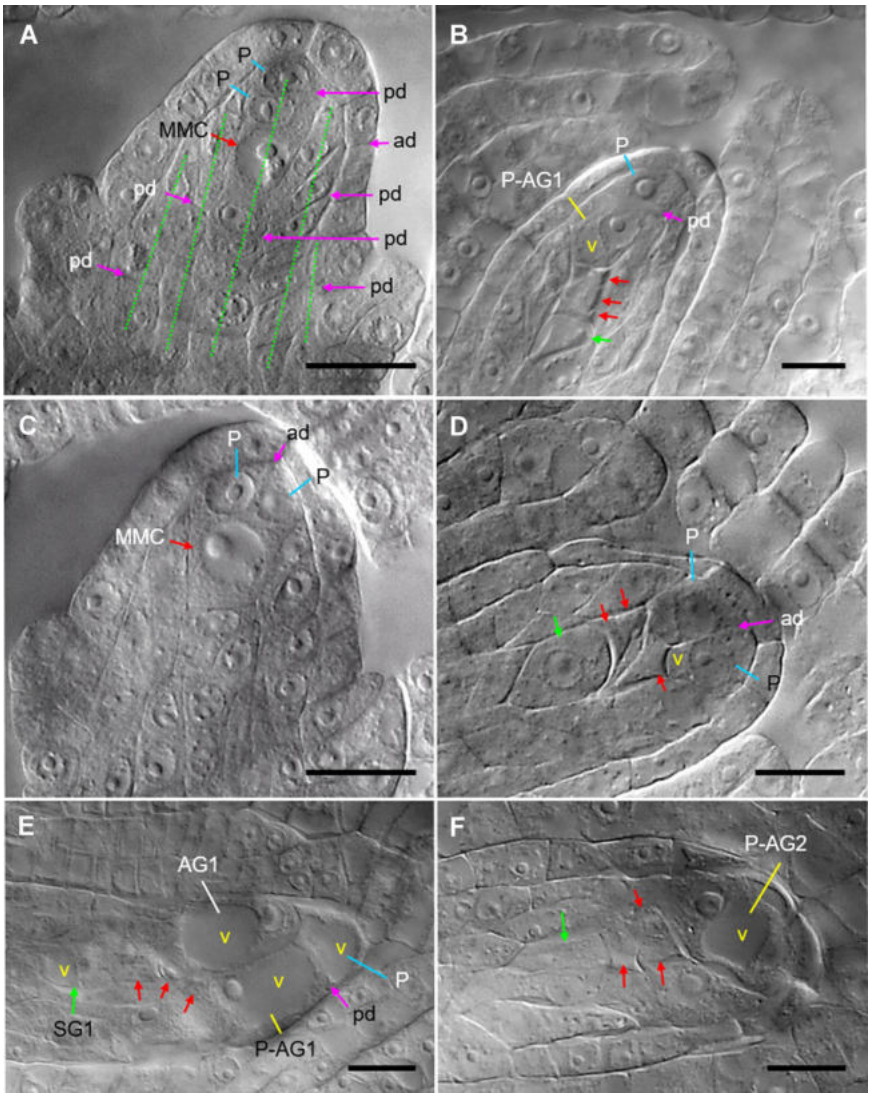

Fig. 5. Sagittal views of sexual megasporogenesis and sexual and aposporous gametophytes in ovules of diploid, triploid and tetraploid *Phoenicaulis cheiranthoides*. **A**, Megaspore mother cell (MMC) staged ovule from the tetraploid Big Indian cytotype. Integument buds and five central columns of nucellar cells are visible (dotted green lines). Cell divisions in these columns are periclinal. The MMC is separated from the nucellar epidermis by two parietal cells that formed by a periclinal division of the original parietal cell (see text). Anticlinal division planes of the nucellar epidermis are also visible. **B,** Tetrad staged ovule from the diploid Lobdell Lake cytotype. Integuments have enclosed the nucellus. The tetrad is separated from the nucellar epidermis by two parietal cells that formed by a periclinal division of the original parietal cell. The proximal cell has initiated aposporous gametophyte formation (enlarged and vacuolate). **C,** MMC staged ovule of the tetraploid Angel Lake cytotype with integument buds visible. The MMC is separated from the nucellar epidermis by two parietal cells that formed by an anticlinal division of the original parietal cell. **D,** Tetrad staged ovule of the triploid Masonic Mnt. cytotype. Integuments have enclosed the nucellus. The tetrad is separated from the nucellar epidermis by two parietal cells that formed by an anticlinal division of the original parietal cell. The lower parietal cell has initiated vacuolation. **E,** Early, 1-nucleate sexual gametophyte staged ovule of the diploid Lobdell Lake cytotype. Integuments have enclosed the nucellus. The tetrad is separated from the nucellar epidermis by two parietal cells that formed by a periclinal division of the original parietal cell. The proximal parietal cell has initiated aposporous gametophyte formation. A second aposporous gametophyte is seen above the proximal parietal cell, which is of nucellar origin. It is actively consuming the degenerating remnants of the tetrad. **F,** T-tetrad staged ovule of the diploid Lobdell Lake cytotype. Integuments have enclosed the nucellus. The tetrad is separated from the nucellar epidermis by a single parietal cell that is developing into a 2–4 nucleate aposporous gametophyte. AG1, unreduced 1-nucleate aposporous gametophyte; ad, anticlinal cell division; MMC, megaspore mother cell; P, parietal cell; pd, periclinal cell division; P-AG1 or 2, 1- or 2-nucleate aposporous gametophyte from a parietal cell; SG1 or 2, reduced 1- or 2-nucleate gametophyte; unlabeled red arrows, degenerating megaspores; unlabeled green arrows, surviving megaspores, most of which were degenerating; v, vacuole. Scale bars, 20 μm.

ovules (Bocher, 1951; Naumova et al., 2001; Carman et al., 2019), parietal tissue has not been reported in *Boechera* ovules. Hence, the positioning of the MMC deeper within the ovule through the formation of parietal tissue, if found to be consistent across the *Phoenicaulis* diversity, would represent an additional characteristic that distinguishes *Phoenicaulis* from *Boechera*. Interestingly, the parietal cells and tissues of *P. cheiranthoides* ovules were susceptible to aposporous gametophyte formation, perhaps more so than neighboring nucellar cells (Figs. 5B, 5D–5F, S1, S2).

Apospory and diplospory are common in *Boechera* (Carman et al., 2019), but only apospory, accompanied by complete meioses (producing tetrads of reduced megaspores), was observed among our limited sampling of *P. cheiranthoides*. Polarity in the aposporous gametophytes was achieved early, as detected by large vacuoles that separated nuclei to opposite poles (Fig. 5F). Unexpectedly, the frequency of apospory was higher in the diploids and tetraploids, approaching 100%, than in the triploid, ca. 35% (Fig. 4). Apparently, abnormal meioses, associated with triploidy, do not trigger apospory in *P. cheiranthoides*. On the contrary, sexual gametophytes forming from surviving megaspores were common in ovules of the triploid, though most of these were probably sterile due to aneuploidy. Accordingly, most viable seeds produced by the triploids are probably of aposporous origin.

Acknowledgements

This article is dedicated to Dr. Ihsan A. Al-Shehbaz (Missouri Botanic Garden) on the occasion of his 80th birthday. This work was supported by Czech Ministry of Education, Youth and Sports within the program INTER-EXCELLENCE (project No. LTAUSA17002), by the CEITEC 2020 project (grant No. LQ1601 to MAL), the Utah Agricultural Experiment Station project awards, Utah State University, Logan to JC, and the U. S. National Science Foundation (award DEB-0816560 to MDW).

References

Alexander MP. 1969. Differential staining of aborted and nonaborted pollen. *Stain Technology* 44: 117–122.

Alexander PJ, Windham MD, Beck JB, Al-Shehbaz IA, Allphin L, Bailey CD. 2013. Molecular phylogenetics and taxonomy of the genus *Boechera* and related genera (Brassicaceae: Boechereae). *Systematic Botany* 38: 192–209.

Al-Shehbaz IA. 2010. *Phoenicaulis*. In: Flora of North America Editorial Committee ed. *Flora of North America North of Mexico*. Oxford: Oxford University Press. 415.

Al-Shehbaz IA. 2012. A generic and tribal synopsis of the Brassicaceae (Cruciferae). *Taxon* 61: 931–954.

Asker SE, Jerling L. 1992. *Apomixis in plants*. Boca Raton, FL: CRC Press, Inc.

Bocher TW. 1951. Cytological and embryological studies in the amphi-apomictic *Arabis holboellii* complex. *Det Kongelige Danske Videnskabernes Selskab. Biologiske Skrifter* 6: 1–59.

Carman JG. 1997. Asynchronous expression of duplicate genes in angiosperms may cause apomixis, bispory, tetraspory, and polyembryony. *Biological Journal of the Linnan Society* 61: 51–94.

Carman JG. 2007. Do duplicate genes cause apomixis. In: Horandl E, Grossniklaus U, van Dijk PJ, Sharbel TF eds. *Apomixis: Evolution, mechanisms and perspectives*. Liechtenstein: A. R. G. Gantner Verlag K. G.

Carman JG, Mateo de Arias M, Gao L, Zhao X, Kowallis B, Sherwood DA, Srivastava MK, Dwivedi KK, Price B, Watts L, Windham MD. 2019. Apospory in addition to diplospory is common in *Boechera* where it may facilitate speciation by recombination-driven apomixis-to-sex reversals. *Frontiers in Plant Science* 10: 724.

Crane CF. 2001. Classification of apomixis mechanisms. In: Savidan Y, Carman JG, Dresselhaus T eds. *The flowering of apomixis: From mechanisms to genetic engineering*. Mexico, D.F.: CIMMYT, IRD, European Commission DG VI (FAIR).

Crane CF, Carman JG. 1987. Mechanisms of apomixis in *Elymus rectisetus* from eastern Australia and New Zealand. *American Journal of Botany* 74: 477–496.

Dwivedi KK, Roche DJ, Clemente TE, Ge ZX, Carman JG. 2014. The OCL3 promoter from *Sorghum bicolor* directs gene expression to abscission and nutrient-transfer zones at the bases of floral organs. *Annals of Botany* 114: 489–498.

Ellerstrom S. 1983. Apomictic progeny from *Raphanobrassica*. *Hereditas* 99: 315.

Ellerstrom S, Zagorcheva L. 1977. Sterility and apomictic embryo-sac formation in *Raphanobrassica*. *Hereditas* 87: 107–119.

Hand ML, Koltunow AM. 2014. The genetic control of apomixis: Asexual seed formation. *Genetics* 197: 441–450.

Hojsgaard D, Klatt S, Baier R, Carman JG, Horandl E. 2014. Taxonomy and biogeography of apomixis in angiosperms and associated biodiversity characteristics. *Critical Reviews in Plant Science* 33: 414–427.

Ijdo JW, Wells RA, Baldini A, Reeders ST. 1991. Improved telomere detection using a telomere repeat probe (TTAGGG)*n* generated by PCR. *Nucleic Acids Research* 19: 4780.

Johri BM, Ambegaokar KB, Srivastava PS. 1992. *Comparative embryology of angiosperms*. New York: Springer-Verlag. 1.

Jordon-Thaden I, Koch MA. 2012. Detection of apomixis in an octoploid, alpine species, *Draba oligosperma* (Brassicaceae). International Plant and Animal Genome Conference XX, San Diego, CA. Available from https://pag.confex.com/pag/xx/webprogram/Paper1684.html.

Kantama L, Sharbel TF, Schranz ME, Mitchell-Olds T, de Vries S, de Jong H. 2007. Diploid apomicts of the *Boechera holboellii* complex display large-scale chromosome substitutions and aberrant chromosomes. *Proceedings of the National Academy of Sciences USA* 104: 14026–14031.

Lysak MA, Mandáková T, Schranz ME. 2016. Comparative paleogenomics of crucifers: Ancestral genomic blocks revisited. *Current Opinions in Plant Biology* 30: 108–115.

Mandáková T, Lysak MA. 2016a. Chromosome preparation for cytogenetic analyses in *Arabidopsis*. *Current Protocols in Plant Biology* 1: 43–51.

Mandáková T, Lysak MA. 2016b. Painting of *Arabidopsis* chromosomes with chromosome-specific BAC clones. *Current Protocols in Plant Biology* 1: 359–371.

Mandáková T, Pouch M, Harmanová K, Zhan SH, Mayrose I, Lysak MA. 2017. Multispeed genome diploidization and diversification after an ancient allopolyploidization. *Molecular Ecology* 26: 6445–6462.

Mandáková T, Schranz ME, Sharbel TF, de Jong H, Lysak MA. 2015. Karyotype evolution in apomictic *Boechera* and the origin of the aberrant chromosomes. *Plant Journal* 82: 785–793.

Mosquin T, Hayley DE. 1966. Chromosome numbers and taxonomy of some Canadian Arctic plants. *Canadian Journal of Botany* 44: 1209–1218.

Mulligan GA. 1966. Chromosome numbers of the family Crucifereae III. *Canadian Journal of Botany* 44: 309–319.

Mulligan GA, Findlay JN. 1970. Sexual reproduction and agamospermy in the genus *Draba*. *Canadian Journal of Botany* 48: 269–271.

Naumova TN, van der Laak J, Osadtchiy J, Matzk F, Kravtchenko A, Bergervoet J, Ramulu KS, Boutilier K. 2001. Reproductive development in apomictic populations of *Arabis holboellii* (Brassicaceae). *Sexual Plant Reproduction* 14: 195–200.

Nikolov LA, Shushkov P, Nevado B, Gan X, Al-Shehbaz IA, Filatov D, Bailey CD, Tsiantis M. 2019. Resolving the backbone of the Brassicaceae phylogeny for investigating trait diversity. *New Phytologist* 222: 1638–1651.

Nogler GA. 1984. Gametophytic apomixis. In: Johri BM ed. *Embryology of angiosperms*. New York: Springer-Verlag.

Rojek J, Kapusta M, Kozieradzka-Kiszkurno M, Majcher D, Gorniak M, Sliwinska E, Sharbel TF, Bohdanowicz J. 2018. Establishing the cell biology of apomictic reproduction in diploid *Boechera stricta* (Brassicaceae). *Annals of Botany* 122: 513–539.

Sharbel TF, Voigt ML, Corral JM, Galla G, Kumlehn J, Klukas C, Schreiber F, Vogel H, Rotter B. 2010. Apomictic and sexual ovules of *Boechera* display heterochronic global gene expression patterns. *The Plant Cell* 22: 655–671.

Sharbel TF, Voigt ML, Mitchell-Olds T, Kantama L, de Jong H. 2004. Is the aneuploid chromosome in an apomictic *Boechera holboellii* a genuine B chromosome? *Cytogenetic and Genome Research* 106: 173–183.

Taskin KM, Turgut K, Scott RJ. 2004. Apomictic development in *Arabis gunnisoniana*. *Israel Journal of Plant Science* 52: 155–160.

Supplementary Material

The following supplementary material is available online for this article at http://onlinelibrary.wiley.com/doi/10.1111/jse.12555/suppinfo:

Table S1. Pollen fertility in the three cytotypes of *Phoenicaulis cheiranthoides*.

Fig. S1. Sagittal views of sexual megasporogenesis and sexual and aposporous gametophytes in ovules of diploid and triploid *Phoenicaulis cheiranthoides*.

Fig. S2. Sagittal views of sexual megasporogenesis and sexual and aposporous gametophytes in ovules of tetraploid *Phoenicaulis cheiranthoides*.

Fig. S3. Pollen fertility in the three cytotypes of *Phoenicaulis cheiranthoides*.